

# Simulating Diffusion Bridges with Score Matching

Jeremy Heng<sup>\*†</sup>   Valentin De Bortoli<sup>‡</sup>   Arnaud Doucet<sup>§</sup>   James Thornton<sup>§</sup>

November 1, 2022

## Abstract

We consider the problem of simulating diffusion bridges, which are diffusion processes that are conditioned to initialize and terminate at two given states. The simulation of diffusion bridges has applications in diverse scientific fields and plays a crucial role in the statistical inference of discretely-observed diffusions. This is known to be a challenging problem that has received much attention in the last two decades. This article contributes to this rich body of literature by presenting a new avenue to obtain diffusion bridge approximations. Our approach is based on a backward time representation of a diffusion bridge, which may be simulated if one can time-reverse the unconditioned diffusion. We introduce a variational formulation to learn this time-reversal with function approximation and rely on a score matching method to circumvent intractability. Another iteration of our proposed methodology approximates the Doob’s  $h$ -transform defining the forward time representation of a diffusion bridge. We discuss algorithmic considerations and extensions, and present numerical results on an Ornstein–Uhlenbeck process, a model from financial econometrics for interest rates, and a model from genetics for cell differentiation and development to illustrate the effectiveness of our approach.

**Keywords:** Diffusion; Diffusion bridge; Score matching; Stochastic differential equation; Time-reversal.

## 1 Introduction

Diffusion processes have been used extensively in mathematical and natural sciences. A diffusion process  $X = (X_t)_{t \in [0, T]}$  in  $\mathbb{R}^d$  is defined by the stochastic differential equation

$$dX_t = f(t, X_t)dt + \sigma(t, X_t)dW_t, \quad (1)$$

where  $f : [0, T] \times \mathbb{R}^d \rightarrow \mathbb{R}^d$  is a drift function,  $\sigma : [0, T] \times \mathbb{R}^d \rightarrow \mathbb{R}^{d \times d}$  is a diffusion coefficient, and  $W = (W_t)_{t \in [0, T]}$  is a  $d$ -dimensional Brownian motion. We suppose  $f$  and  $\sigma$  are sufficiently regular to induce a unique weak solution and  $\Sigma(t, x_t) = (\sigma\sigma)^\top(t, x_t)$  is uniformly positive definite for all  $(t, x_t) \in [0, T] \times \mathbb{R}$ . For any  $0 \leq s < t \leq T$ , we denote the transition density of (1) with respect to the Lebesgue measure on  $\mathbb{R}^d$  as  $p(t, x_t \mid s, x_s)$  and assume that it is positive for ease of exposition.

<sup>\*</sup>ESSEC Business School, Singapore 139408, Singapore

<sup>†</sup>Corresponding author: heng@essec.edu

<sup>‡</sup>Center for Science of Data, ENS Ulm, Paris 75005, France

<sup>§</sup>Department of Statistics, University of Oxford, Oxford OX1 3LB, U.K.

While the numerical simulation of  $X$  can be routinely handled by time-discretization schemes (Kloeden and Platen, 1992), the task of simulating  $X$  initialized at  $X_0 = x_0$  and conditioned to terminate at  $X_T = x_T$  is a challenging problem that has received much attention in the last two decades.

Simulating the conditioned process  $X^* = (X_t^*)_{t \in [0, T]}$ , commonly referred to as a diffusion bridge, has applications in diverse fields such as computational chemistry (Bolhuis et al., 2002; Wang et al., 2020), financial econometrics (Elerian et al., 2001; Durham and Gallant, 2002), genetics (Wang et al., 2011), and shape analysis (Arnaudon et al., 2022). When performing statistical inference for parameters of  $f$  and  $\sigma$  in the case where  $X$  is observed at discrete time points, diffusion bridge simulation is a crucial tool that allows one to impute missing paths between observations within an expectation-maximization algorithm or a Gibbs sampler (Pedersen, 1995; Roberts and Stramer, 2001; Eraker, 2001; Beskos et al., 2006; Golightly and Wilkinson, 2008; van der Meulen and Schauer, 2017).

By Doob’s  $h$ -transform (Rogers and Williams, 2000, p. 83), it is well-known that  $X^*$  satisfies

$$dX_t^* = \{f(t, X_t^*) + \Sigma(t, X_t^*) \nabla \log h(t, X_t^*)\} dt + \sigma(t, X_t^*) dW_t, \quad X_0^* = x_0, \quad (2)$$

where  $h(t, x_t) = p(T, x_T | t, x_t)$  and  $\nabla$  denotes the gradient operator. The term  $\Sigma(t, x_t) \nabla \log h(t, x_t)$  forces the conditioned process towards the terminal condition  $X_T^* = x_T$ . As the transition density and hence its logarithmic gradient is intractable for most diffusions, exploiting this result to simulate diffusion bridges is highly non-trivial. To this end, one can characterize  $h$  as the solution of the backward Kolmogorov equation

$$\partial_t h(t, x_t) + (\mathcal{L}h)(t, x_t) = 0, \quad (3)$$

with terminal condition at time  $T$  given by the Dirac measure at  $x_T$ , where  $\mathcal{L}$  denotes the generator of  $X$ . Equation (3) reveals that  $h$  propagates information about the terminal constraint backwards in time. However, numerical resolution of this partial differential equation is particularly challenging due to the singularity at time  $T$ , and computationally demanding when the dimension  $d$  is large (Wang et al., 2020). Furthermore, one must run a solver for every pair of conditioned states  $(x_0, x_T)$  considered.

A common approach to address these difficulties is to simulate a proposal bridge process  $X^\circ = (X_t^\circ)_{t \in [0, T]}$ , satisfying  $dX_t^\circ = f^\circ(t, X_t^\circ) dt + \sigma(t, X_t^\circ) dW_t$  with  $X_0^\circ = x_0$ . One constructs  $f^\circ : [0, T] \times \mathbb{R}^d \rightarrow \mathbb{R}^d$  using a tractable approximation of (2), and corrects for the discrepancy using importance sampling or an independent Metropolis–Hastings algorithm (Papaspiliopoulos and Roberts, 2012; Elerian et al., 2001). The simple choice  $f^\circ(t, x_t) = f(t, x_t)$  typically performs poorly as it does not take the constraint  $X_T = x_T$  into account (Pedersen, 1995). The drift of a Brownian bridge  $f^\circ(t, x_t) = (x_T - x_t)/(T - t)$  has been considered in several works (Durham and Gallant, 2002; Delyon and Hu, 2006; Stramer and Yan, 2007; Papaspiliopoulos et al., 2013), and improved by Whitaker et al. (2017) using an innovative decomposition of the process into deterministic and stochastic parts. Clark (1990) followed by Delyon and Hu (2006) studied the choice  $f^\circ(t, x_t) = f(t, x_t) + (x_T - x_t)/(T - t)$  that incorporates the dynamics of the original process  $X$ . To introduce more flexibility and better mimic the structure of (2), Schauer et al. (2017) proposed setting  $f^\circ(t, x_t) = f(t, x_t) + \Sigma(t, x_t) \nabla \log \tilde{h}(t, x_t)$ , where  $\tilde{h}(t, x_t) = \tilde{p}(T, x_T | t, x_t)$  is an analytically tractable transition density of an auxiliary process. For tractability, the latter is typically chosen from the class of linear processes and can be optimized to get the best approximation within this class (van der Meulen and Schauer, 2017). Other Markov chain Monte

Carlo approaches include Gibbs sampling (Eraker, 2001), Langevin-type stochastic partial differential equations (Stuart et al., 2004; Beskos et al., 2008), and piecewise deterministic Monte Carlo (Bierkens et al., 2021).

The exact simulation algorithms developed in Beskos and Roberts (2005) and Beskos et al. (2006) can be employed to sample diffusion bridges without any time-discretization error. However, these elegant methods are limited to the class of diffusion processes that can be transformed to have unit diffusion coefficient. Bladt and Sørensen (2014) and Bladt et al. (2016) devised an ingenious methodology to simulate diffusion bridges based on coupling and time-reversal of diffusions. Their proposed method is applicable to the class of ergodic diffusions with an invariant density that is either explicitly known or numerically approximated. Closely related approaches include sequential Monte Carlo algorithms that resample using backward information filter approximations (Guarniero, 2017), information from backward pilot paths (Lin et al., 2010), or guided weight functions (Del Moral and Murray, 2015). The main idea underlying these works is the representation of the diffusion bridge in (2) and (3).

This work contributes to this rich body of literature by presenting a new avenue to obtain diffusion bridge approximations. In Section 2.1, we begin by examining the dynamics of the time-reversed bridge process  $X^*$ , which amounts to a time-reversal of (1). Section 2.2 introduces a variational formulation to learn this time-reversal using function approximation and a score matching method (Vincent, 2011). In Section 2.3, we explain how another iteration of this methodology approximates the Doob’s  $h$ -transformed process in (2). Our approach is widely applicable and can be used to construct proposal bridge processes within existing frameworks. Lastly, in Section 3 we illustrate computational improvements over common choices of proposal bridge processes on three numerical examples. A Python package is available on [GitHub](#).

## 2 Diffusion bridges

### 2.1 Time-reversed bridge process

It can be shown that the time-reversed bridge process  $Z^* = (Z_t^*)_{t \in [0, T]} = (X_{T-t}^*)_{t \in [0, T]}$  satisfies

$$dZ_t^* = b(t, Z_t^*)dt + \sigma(T - t, Z_t^*)dB_t, \quad Z_0^* = x_T, \quad (4)$$

with drift function  $b(t, z_t) = -f(T - t, z_t) + \Sigma(T - t, z_t)s(T - t, z_t) + \nabla \cdot \Sigma(T - t, z_t)$ , another standard Brownian motion  $B = (B_t)_{t \in [0, T]}$ ,  $s(t, x_t) = s^*(t, x_t) - \nabla \log h(t, x_t)$ , and  $\nabla \cdot \Sigma(t, x) = (\sum_{j=1}^d \partial_{x_j} \Sigma^{1,j}(t, x), \dots, \sum_{j=1}^d \partial_{x_j} \Sigma^{d,j}(t, x))$  is the divergence of  $\Sigma$ . Here  $s^*(t, x_t) = \nabla \log p^*(t, x_t)$  denotes the score of the marginal density  $p^*(t, x_t)$  of the diffusion bridge process  $X_t^*$  at time  $t \in (0, T)$ . We refer readers to Haussmann and Pardoux (1986) and Millet et al. (1989) for conditions under which the representation in (4) holds. By the Markov property, we have the relation

$$p^*(t, x_t) = p\{t, x_t \mid (0, x_0), (T, x_T)\} = \frac{p(t, x_t \mid 0, x_0)h(t, x_t)}{p(T, x_T \mid 0, x_0)}, \quad (5)$$

as  $h(t, x_t) = p(T, x_T \mid t, x_t)$ . This implies that  $s(t, x_t) = \nabla \log p(t, x_t \mid 0, x_0)$  is simply the score of the transition density of  $X$ .

Exploiting this backward time representation to derive diffusion bridge approximations is also highly non-trivial due to the intractability of the transition density  $\eta(t, x_t) = p(t, x_t | 0, x_0)$ , which is now characterized by the forward Kolmogorov equation  $\partial_t \eta(t, x_t) + (\mathcal{F}\eta)(t, x_t) = 0$ , with initial condition at time 0 given by the Dirac measure at  $x_0$  and  $\mathcal{F}$  denotes the Fokker–Planck operator of  $X$ . Numerical resolution of  $\eta$  using partial differential equation solvers also suffers from the same difficulties as (3). A key observation is that (4) can be understood as first setting  $Z_0^* = x_T$  to satisfy the terminal constraint, and then evolving  $Z^*$  using the time-reversal of (1). Due to the influence of the score  $s(t, x_t)$ , the process will end at the initial constraint  $Z_T^* = x_0$  by construction. This connection between simulation of a diffusion bridge and time-reversal of its original diffusion process will form the basis of our score approximation.

## 2.2 Learning time-reversal with score matching

We introduce a variational formulation to learn the time-reversal of (1), involving path measures on the space of continuous functions from  $[0, T]$  to  $\mathbb{R}^d$ , equipped with the cylinder  $\sigma$ -algebra. Let  $\mathbb{P}^{x_0}$  denote the path measure induced by (1) with  $X_0 = x_0$ , and  $\mathbb{Q}_\phi^{x_0}$  be the path measure induced by a time-reversed process  $Z = (Z_t)_{t \in [0, T]}$  satisfying

$$dZ_t = b_\phi(t, Z_t)dt + \sigma(T - t, Z_t)dB_t, \quad Z_0 \sim p(T, dx_T | 0, x_0), \quad (6)$$

with drift function  $b_\phi(t, z_t) = -f(T - t, z_t) + \Sigma(T - t, z_t)s_\phi(T - t, z_t) + \nabla \cdot \Sigma(T - t, z_t)$  that mimics the form of  $b(t, z_t)$  in (4). Here  $s_\phi : [0, T] \times \mathbb{R}^d \rightarrow \mathbb{R}^d$  represents a function approximation of the score  $s(t, x_t)$  that depends on parameters  $\phi \in \Phi$  to be optimized. We shall measure the score approximation error as

$$e(\phi) = E^{x_0} \left\{ \int_0^T \|s_\phi(t, X_t) - s(t, X_t)\|_{\Sigma(t, X_t)}^2 dt \right\}, \quad (7)$$

where  $E^{x_0}$  denotes expectation with respect to  $\mathbb{P}^{x_0}$  and  $\|\cdot\|_A$  denotes the Euclidean norm weighted by a positive definite  $A \in \mathbb{R}^{d \times d}$ .

Let  $d\mathbb{P}^{x_0}/d\mathbb{Q}_\phi^{x_0}$  denote the Radon–Nikodym derivative of  $\mathbb{P}^{x_0}$  with respect to  $\mathbb{Q}_\phi^{x_0}$ . We consider minimizing the Kullback–Leibler divergence  $\text{KL}(\mathbb{P}^{x_0} | \mathbb{Q}_\phi^{x_0}) = E^{x_0} \{\log d\mathbb{P}^{x_0}/d\mathbb{Q}_\phi^{x_0}(X)\}$ . The following result gives an expression of this objective and shows that the process  $Z$  will end at the initial constraint  $Z_T = x_0$  if the score approximation error is finite.

**Proposition 1.** *Assuming  $e(\phi) < \infty$ , we have  $\text{KL}(\mathbb{P}^{x_0} | \mathbb{Q}_\phi^{x_0}) = e(\phi)/2$  and  $Z_T = x_0$  holds  $\mathbb{Q}_\phi^{x_0}$ -almost surely.*

Although this clearly relates learning the time-reversal of (1) with approximation of the score  $s(t, x_t)$ , its form is not amenable to optimization. The following result gives an alternative and practical expression by adapting the idea of denoising score matching (Vincent, 2011) to our setting.

**Proposition 2.** *For any partition  $(t_m)_{m=0}^M$  of the interval  $[0, T]$ , we have  $\text{KL}(\mathbb{P}^{x_0} | \mathbb{Q}_\phi^{x_0}) = L(\phi) + C$  if  $e(\phi) < \infty$ , where  $C$  is a constant independent of  $\phi \in \Phi$ , the loss function is defined as*

$$L(\phi) = \frac{1}{2} \sum_{m=1}^M \int_{t_{m-1}}^{t_m} E^{x_0} \left\{ \|s_\phi(t, X_t) - g(t_{m-1}, X_{t_{m-1}}, t, X_t)\|_{\Sigma(t, X_t)}^2 \right\} dt, \quad (8)$$

and  $g(s, x_s, t, x_t) = \nabla \log p(t, x_t | s, x_s)$  for  $0 \leq s < t \leq T$  and  $x_s, x_t \in \mathbb{R}^d$ .

Therefore minimizing the Kullback–Leibler divergence  $\text{KL}(\mathbb{P}^{x_0} | \mathbb{Q}_\phi^{x_0})$  is equivalent to minimizing the loss function  $L(\phi)$ . This allows us to circumvent the intractable score  $s(t, x_t)$  by working with  $g(t_{m-1}, x_{t_{m-1}}, t, x_t)$ , the score of the transition density  $p(t, x_t | t_{m-1}, x_{t_{m-1}})$ . Although the latter is also intractable, approximations can be made when the sub-interval  $[t_{m-1}, t_m]$  is sufficiently small. For example, under the Euler–Maruyama scheme (Kloeden and Platen, 1992, p. 340) with stepsize  $\delta t = T/M$ ,

$$g(t_{m-1}, x_{t_{m-1}}, t_m, x_{t_m}) \approx -(\delta t)^{-1} \Sigma^{-1}(t_{m-1}, x_{t_{m-1}}) \{x_{t_m} - x_{t_{m-1}} - \delta t f(t_{m-1}, x_{t_{m-1}})\}.$$

Hence the loss  $L(\phi)$  can be approximated and minimized using stochastic gradient algorithms by simulating time-discretized paths under (1). The minimal loss of  $L(\phi) = -C$ , achieved when  $s_\phi(t, x_t) = s(t, x_t)$   $\mathbb{P}^{x_0}$ -almost surely, is unknown as the constant  $C$  is typically incomputable. After obtaining the score approximation  $s_\phi$ , we can simulate a proposal bridge  $Z$  from (6) with  $Z_0 = x_T$  and correct it using importance sampling or independent Metropolis–Hastings. Time-discretization considerations and proposal correction procedures are detailed in Appendix C.

In scenarios where one is interested in multiple pairs of conditioned states  $(x_0, x_T)$ , we can extend the above methodology to avoid having to learn multiple score approximations as follows. We let the score approximation  $s_\phi(t, x_t)$  in (6) also depend on the initial condition  $x_0$ , and average the Kullback–Leibler objective  $\text{KL}(\mathbb{P}^{x_0} | \mathbb{Q}_\phi^{x_0})$  with a distribution  $p_0(dx_0)$  on  $\mathbb{R}^d$  that can be sampled from. By applying the arguments of Proposition 2 conditionally on  $X_0 = x_0$ , we obtain a loss function given by averaging (8) over  $p_0(dx_0)$ , which can be minimized using time-discretization and stochastic gradient algorithms.

## 2.3 Learning Doob’s $h$ -transform

It is instructive to consider the time-reversal of (4), which gives

$$dX_t^* = f^*(t, X_t^*)dt + \sigma(t, X_t^*)dW_t, \quad X_0^* = x_0, \quad (9)$$

with drift function  $f^*(t, x_t) = -b(T - t, x_t) + \Sigma(t, x_t)s^*(t, x_t) + \nabla \cdot \Sigma(t, x_t)$ . Using the form of  $b(t, z_t)$  and the relation  $s(t, x_t) = s^*(t, x_t) - \nabla \log h(t, x_t)$ , we can rewrite  $f^*$  as

$$f^*(t, x_t) = f(t, x_t) + \Sigma(t, x_t)\{s^*(t, x_t) - s(t, x_t)\} = f(t, x_t) + \Sigma(t, x_t)\nabla \log h(t, x_t), \quad (10)$$

therefore (9) recovers the Doob’s  $h$ -transform in (2). Although this is to be expected as the reversal of the time-reversed process should recover the original process, it forms the basis of our approximation of (2).

After obtaining an approximation of  $s(t, x_t)$ , another iteration of our proposed methodology can be used to learn a function approximation of  $s^*(t, x_t)$ . For brevity, this is detailed in Appendix B. Plugging in both approximations in (10) then gives an approximation of  $X^*$ , which could be of interest in algorithms where one requires a forward time representation of the proposal bridge process (Lin et al., 2010; Del Moral and Murray, 2015).

## 3 Numerical examples

### 3.1 Preliminaries

As our methodology allows one to employ any function approximator, we harness the flexibility of neural networks and the ease of implementation using modern software to approximate score functions. The choice of neural network and stochastic gradient algorithm is detailed in Appendix D. Optimization times ranged between several seconds to a few minutes on a simple desktop machine and can be reduced with hardware accelerators. As such computational overheads are marginal when deploying proposal bridge processes within an importance sampler with many samples or an independent Metropolis–Hastings algorithm with many iterations, we focus on assessing the quality of our proposals in settings where existing proposal methods are unsatisfactory. The performance measures considered are the importance sampling effective sample size proportion, the acceptance rate of independent Metropolis–Hastings, and the variance of the importance sampling log-transition density estimator or its mean squared error when the true transition density is known. These measures were computed using 1024 samples or iterations, and 100 independent repetitions of each method. We benchmark our approximations of the backward and forward diffusion bridges in (4) and (9) against the forward diffusion method of Pedersen (1995), the modified diffusion bridge of Durham and Gallant (2002), and the Clark–Delyon–Hu proposal bridge process studied by Clark (1990) and Delyon and Hu (2006). Given the difficulty of comparing the wide range of methods for diffusion bridges in a completely fair manner, as their strengths and weaknesses can depend on the specificities of the problem under consideration, we note that our objective is merely to illustrate a new avenue to improve the construction of proposal bridge processes.

### 3.2 Ornstein–Uhlenbeck process

Consider (1) with linear drift function  $f(t, x_t) = -2x_t$ , identity diffusion coefficient  $\sigma(t, x_t) = I_d$ , and the constraints  $x_0 = x_T = (1, \dots, 1)$ . The transition density and score function are explicitly known and used as ground truth. Fig. 1 illustrates the impact of the time horizon  $T$  and dimension  $d$  on algorithmic performance. We observe that our proposal bridge processes offer substantial improvements over existing methods in all settings considered. When comparing our forward and backward diffusion bridge approximations, we notice some accumulation of error, which is to be expected as the forward process is constructed using an additional score approximation. Given this observation, we will only consider the backward process in the following.

### 3.3 Interest rates model

Next, we consider a special case of an interest rates model in Aït-Sahalia and Lo (1998), defined by (1) with  $f(t, x_t) = 4/x_t - x_t$  and  $\sigma(t, x_t) = 1$ . This specification admits a tractable transition density and score function as ground truth, given in terms of modified Bessel functions and its derivative. For each  $T$ , we first learn a single score approximation to handle multiple conditioned states  $(x_0, x_T)$  by minimizing the loss in (8) averaged over initial states  $X_0 = x_0$  from the gamma distribution with shape 5 and rate 2. We visualize our score approximation for  $T = 1$  in Fig. 2, and examine how algorithmic performance depends on  $T$  and  $(x_0, x_T)$  in Fig. 3. While the performance

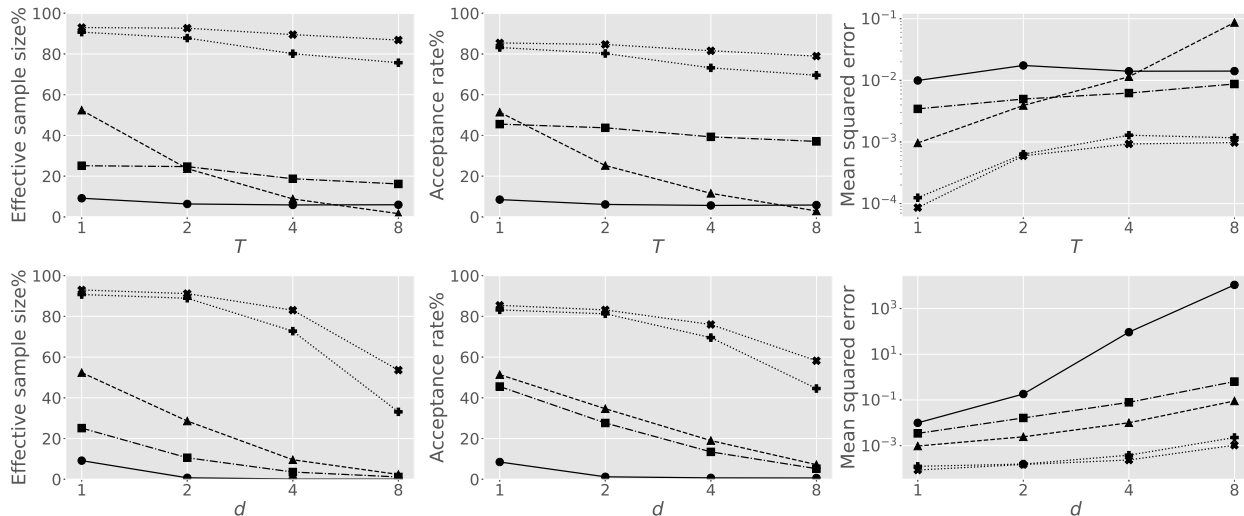


Figure 1: Results for Ornstein–Uhlenbeck example with fixed  $d = 1$  (*first row*) and fixed  $T = 1$  (*second row*). The symbols and lines correspond to our approximations of the backward (*cross-dotted*) and forward (*plus-dotted*) diffusion bridges, the forward diffusion (*circle-solid*), the modified diffusion bridge (*triangle-dashed*), and the Clark–Delyon–Hu bridge (*square-dash-dotted*).

of modified diffusion bridge typically degrades with  $T$ , the forward diffusion and Clark–Delyon–Hu bridge may yield more satisfactory results for specific conditioned states (second column). In contrast, our backward diffusion bridge approximation performs well for all  $T$  considered and when conditioning requires the process to move away from the stable stationary point of  $f$  at  $x = 2$  (first and third columns).

### 3.4 Cell model

We end with a cell differentiation and development model from Wang et al. (2011). Cellular expression levels  $X_t = (X_{t,1}, X_{t,2})$  of two genes are modelled by (1) with  $f = (f_1, f_2)$ , where  $f_i(t, x_t) = x_{t,i}^4 / (2^{-4} + x_{t,i}^4) + 2^{-4} / (2^{-4} + x_{t,j}^4) - x_{t,i}$ , for  $(i, j) \in \{(1, 2), (2, 1)\}$ , describe self-activation, mutual inhibition and inactivation respectively, and  $\sigma(t, x_t) = \sigma_X I_2$  captures intrinsic or external fluctuations. We consider the cell development from the undifferentiated state of  $x_0 = (1, 1)$  to a differentiated state  $x_T = (x_{T,1}, x_{T,2})$  defined by another stable fixed point of  $f$  satisfying  $x_{T,1} < x_{T,2}$ . Fig. 4 displays the performance of all proposal methods to approximate this diffusion bridge. For this application, we observe significant improvement over other methods when the time horizon is long and when the diffusion coefficient  $\sigma_X$  is smaller.

## Acknowledgements

Jeremy Heng was funded by CY Initiative of Excellence (grant “Investissements d’Avenir” ANR-16-IDEX-0008). Valentin De Bortoli and Arnaud Doucet are partly supported by the EPSRC grant CoSInES EP/R034710/1.

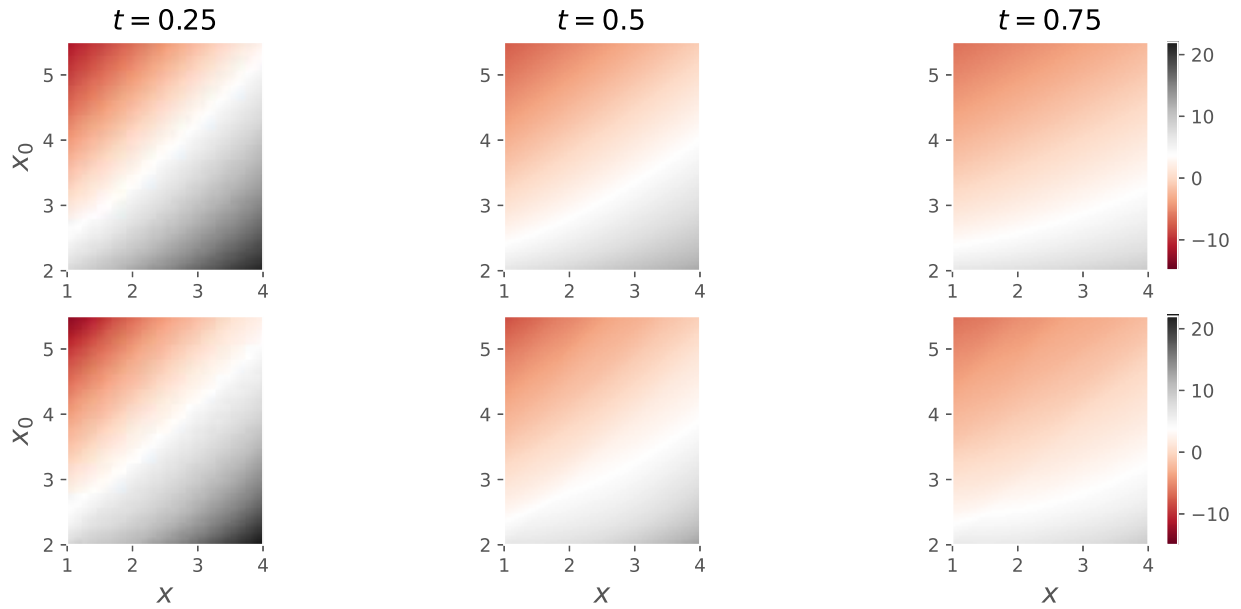


Figure 2: Comparing true score function  $s(t, x)$  (first row) and our function approximation  $s_\phi(t, x)$  (second row) for various time  $t$  and initial condition  $x_0$ .

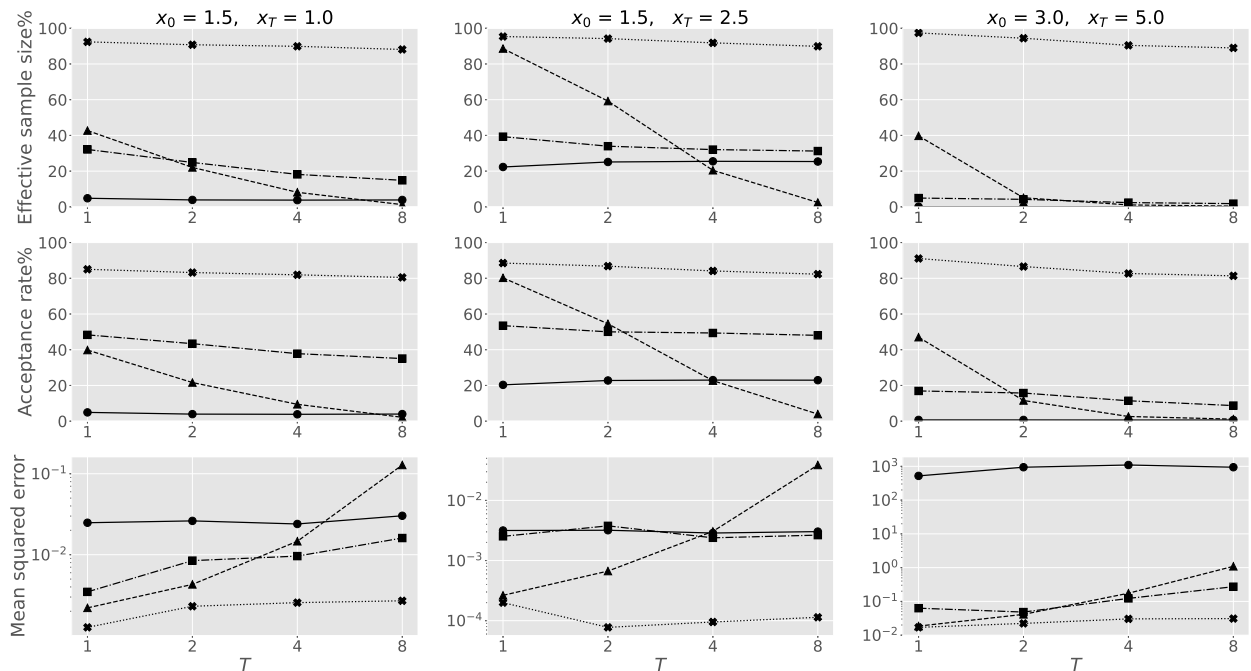


Figure 3: Results for interest rates model for three pairs of conditioned states  $(x_0, x_T)$ . The symbols and lines correspond to our approximation of the backward diffusion bridge (cross-dotted), the forward diffusion (circle-solid), the modified diffusion bridge (triangle-dashed), and the Clark–Delyon–Hu bridge (square-dash-dotted).

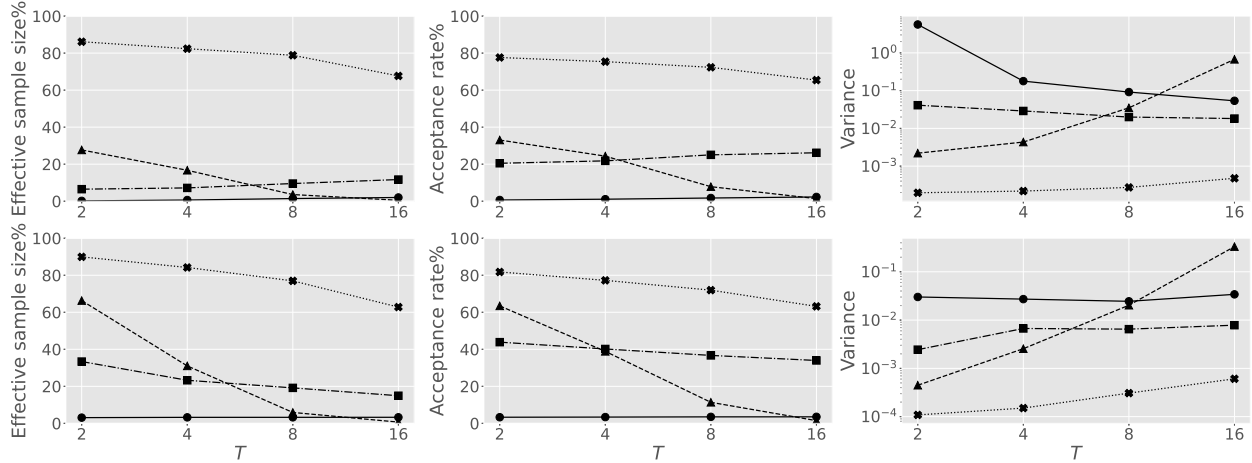


Figure 4: Results for cell model with  $\sigma_X^2 = 0.1$  (first row) and  $\sigma_X^2 = 1$  (second row). The symbols and lines correspond to our approximation of the backward diffusion bridge (cross-dotted), the forward diffusion (circle-solid), the modified diffusion bridge (triangle-dashed), and the Clark–Delyon–Hu bridge (square-dash-dotted).

## References

- Aït-Sahalia, Y. and A. W. Lo (1998). Nonparametric estimation of state-price densities implicit in financial asset prices. *The Journal of Finance* 53(2), 499–547. [6](#), [18](#)
- Andrieu, C., A. Doucet, and R. Holenstein (2010). Particle Markov chain Monte Carlo methods (with discussion). *Journal of the Royal Statistical Society: Series B (Statistical Methodology)* 72(3), 269–342. [16](#)
- Arnaudon, A., F. van der Meulen, M. Schauer, and S. Sommer (2022). Diffusion bridges for stochastic Hamiltonian systems and shape evolutions. *SIAM Journal on Imaging Sciences* 15(1), 293–323. [2](#)
- Beskos, A., O. Papaspiliopoulos, and G. O. Roberts (2006). Retrospective exact simulation of diffusion sample paths with applications. *Bernoulli* 12(6), 1077–1098. [3](#)
- Beskos, A., O. Papaspiliopoulos, G. O. Roberts, and P. Fearnhead (2006). Exact and computationally efficient likelihood-based estimation for discretely observed diffusion processes (with discussion). *Journal of the Royal Statistical Society: Series B (Statistical Methodology)* 68(3), 333–382. [2](#)
- Beskos, A. and G. O. Roberts (2005). Exact simulation of diffusions. *The Annals of Applied Probability* 15(4), 2422–2444. [3](#)
- Beskos, A., G. O. Roberts, A. Stuart, and J. Voss (2008). MCMC methods for diffusion bridges. *Stochastics and Dynamics* 8(03), 319–350. [3](#)
- Bierkens, J., S. Grazi, F. van der Meulen, and M. Schauer (2021). A piecewise deterministic Monte Carlo method for diffusion bridges. *Statistics and Computing* 31(3), 1–21. [3](#)

- Bladt, M., S. Finch, and M. Sørensen (2016). Simulation of multivariate diffusion bridges. *Journal of the Royal Statistical Society: Series B (Statistical Methodology)*, 343–369. [3](#)
- Bladt, M. and M. Sørensen (2014). Simple simulation of diffusion bridges with application to likelihood inference for diffusions. *Bernoulli* 20(2), 645–675. [3](#)
- Bolhuis, P. G., D. Chandler, C. Dellago, and P. L. Geissler (2002). Transition path sampling: Throwing ropes over rough mountain passes, in the dark. *Annual Review of Physical Chemistry* 53(1), 291–318. [2](#)
- Clark, J. M. C. (1990). The simulation of pinned diffusions. In *29th IEEE Conference on Decision and Control*, pp. 1418–1420. IEEE. [2](#), [6](#)
- Del Moral, P. and L. M. Murray (2015). Sequential Monte Carlo with highly informative observations. *SIAM/ASA Journal on Uncertainty Quantification* 3(1), 969–997. [3](#), [5](#)
- Delyon, B. and Y. Hu (2006). Simulation of conditioned diffusion and application to parameter estimation. *Stochastic Processes and their Applications* 116(11), 1660–1675. [2](#), [6](#)
- Durham, G. B. and A. R. Gallant (2002). Numerical techniques for maximum likelihood estimation of continuous-time diffusion processes. *Journal of Business & Economic Statistics* 20(3), 297–338. [2](#), [6](#), [15](#)
- Elerian, O., S. Chib, and N. Shephard (2001). Likelihood inference for discretely observed nonlinear diffusions. *Econometrica* 69(4), 959–993. [2](#), [16](#)
- Eraker, B. (2001). MCMC analysis of diffusion models with application to finance. *Journal of Business & Economic Statistics* 19(2), 177–191. [2](#), [3](#)
- Golightly, A. and D. J. Wilkinson (2008). Bayesian inference for nonlinear multivariate diffusion models observed with error. *Computational Statistics & Data Analysis* 52(3), 1674–1693. [2](#)
- Guarniero, P. (2017). *The Iterated Auxiliary Particle Filter and Applications to State Space Models and Diffusion Processes*. Ph. D. thesis, University of Warwick. [3](#)
- Hausmann, U. G. and E. Pardoux (1986). Time reversal of diffusions. *The Annals of Probability*, 1188–1205. [3](#)
- Kingma, D. P. and J. Ba (2014). Adam: A method for stochastic optimization. *arXiv preprint arXiv:1412.6980*. [17](#)
- Kloeden, P. E. and E. Platen (1992). Stochastic differential equations. In *Numerical Solution of Stochastic Differential Equations*, pp. 103–160. Springer. [2](#), [5](#), [14](#)
- Lin, M., R. Chen, and P. Mykland (2010). On generating Monte Carlo samples of continuous diffusion bridges. *Journal of the American Statistical Association* 105(490), 820–838. [3](#), [5](#), [16](#)
- Middleton, L., G. Deligiannidis, A. Doucet, and P. E. Jacob (2019). Unbiased smoothing using particle independent Metropolis–Hastings. In *International Conference on Artificial Intelligence and Statistics*. PMLR. [16](#)

- Millet, A., D. Nualart, and M. Sanz (1989). Integration by parts and time reversal for diffusion processes. *The Annals of Probability*, 208–238. [3](#)
- Papaspiliopoulos, O. and G. O. Roberts (2012). Importance sampling techniques for estimation of diffusion models. In M. Kessler, A. Lindner, and M. Sorensen (Eds.), *Statistical Methods for Stochastic Differential Equations*, pp. 311–340. Chapman and Hall/CRC. [2](#)
- Papaspiliopoulos, O., G. O. Roberts, and O. Stramer (2013). Data augmentation for diffusions. *Journal of Computational and Graphical Statistics* 22(3), 665–688. [2](#), [15](#)
- Pedersen, A. R. (1995). Consistency and asymptotic normality of an approximate maximum likelihood estimator for discretely observed diffusion processes. *Bernoulli*, 257–279. [2](#), [6](#)
- Roberts, G. O. and O. Stramer (2001). On inference for partially observed nonlinear diffusion models using the Metropolis–Hastings algorithm. *Biometrika* 88(3), 603–621. [2](#)
- Rogers, L. C. G. and D. Williams (2000). *Diffusions, Markov processes and Martingales: Volume 2: Itô Calculus*, Volume 2. Cambridge university press. [2](#), [12](#)
- Schauer, M., F. Van Der Meulen, and H. Van Zanten (2017). Guided proposals for simulating multi-dimensional diffusion bridges. *Bernoulli* 23(4A), 2917–2950. [2](#)
- Stramer, O. and J. Yan (2007). On simulated likelihood of discretely observed diffusion processes and comparison to closed-form approximation. *Journal of Computational and Graphical Statistics* 16(3), 672–691. [2](#)
- Stuart, A. M., J. Voss, and P. Wilberg (2004). Conditional path sampling of SDEs and the Langevin MCMC method. *Communications in Mathematical Sciences* 2(4), 685–697. [3](#)
- van der Meulen, F. and M. Schauer (2017). Bayesian estimation of discretely observed multi-dimensional diffusion processes using guided proposals. *Electronic Journal of Statistics* 11(1), 2358–2396. [2](#)
- Vaswani, A., N. Shazeer, N. Parmar, J. Uszkoreit, L. Jones, A. N. Gomez, Ł. Kaiser, and I. Polosukhin (2017). Attention is all you need. In *Advances in Neural Information Processing Systems*, pp. 5998–6008. [17](#)
- Vincent, P. (2011). A connection between score matching and denoising autoencoders. *Neural Computation* 23(7), 1661–1674. [3](#), [4](#)
- Wang, J., K. Zhang, L. Xu, and E. Wang (2011). Quantifying the Waddington landscape and biological paths for development and differentiation. *Proceedings of the National Academy of Sciences* 108(20), 8257–8262. [2](#), [7](#)
- Wang, S., D. Ramkrishna, and V. Narsimhan (2020). Exact sampling of polymer conformations using Brownian bridges. *The Journal of Chemical Physics* 153(3), 034901. [2](#)
- Whitaker, G. A., A. Golightly, R. J. Boys, and C. Sherlock (2017). Improved bridge constructs for stochastic differential equations. *Statistics and Computing* 27(4), 885–900. [2](#)

## A Proofs of Propositions 1 and 2

In the following, we write  $\langle x, y \rangle_A = x^\top A y$  for the inner product of  $x, y \in \mathbb{R}^d$  weighted by a positive definite matrix  $A \in \mathbb{R}^{d \times d}$  and  $\|x\|_A = \sqrt{\langle x, x \rangle_A}$  for the induced weighted Euclidean norm.

*Proof of Proposition 1.* It follows from Section 2.1 that the path measure  $\mathbb{P}^{x_0}$  is also induced by the backward process  $Z = (Z_t)_{t \in [0, T]} = (X_{T-t})_{t \in [0, T]}$  satisfying

$$dZ_t = b(t, Z_t)dt + \sigma(T-t, Z_t)dB_t, \quad Z_0 \sim p(T, dx_T | 0, x_0). \quad (11)$$

Using Girsanov's theorem (Rogers and Williams, 2000, p. 79) and Equations (11) and (6), the Radon–Nikodym derivative of  $\mathbb{P}^{x_0}$  with respect to  $\mathbb{Q}_\phi^{x_0}$  is

$$\frac{d\mathbb{P}^{x_0}}{d\mathbb{Q}_\phi^{x_0}}(Z) = \exp \left\{ -\frac{1}{2} \int_0^T \|(b - b_\phi)(t, Z_t)\|_{\Sigma^{-1}(T-t, Z_t)}^2 dt + \int_0^T (b - b_\phi)(t, Z_t)^\top (\Sigma^{-1} \sigma)(T-t, Z_t) dB_t \right\}.$$

By properties of Itô integrals, the form of  $b(t, z_t)$  and  $b_\phi(t, z_t)$ , and the identity  $\|Ax\|_{A^{-1}}^2 = \|x\|_A^2$  for a positive definite matrix  $A \in \mathbb{R}^{d \times d}$  and  $x \in \mathbb{R}^d$ , we can write the Kullback–Leibler divergence as

$$\text{KL}(\mathbb{P}^{x_0} | \mathbb{Q}_\phi^{x_0}) = \frac{1}{2} E^{x_0} \left\{ \int_0^T \|s_\phi(t, X_t) - s(t, X_t)\|_{\Sigma(t, X_t)}^2 dt \right\} = \frac{1}{2} e(\phi). \quad (12)$$

Hence  $\text{KL}(\mathbb{P}^{x_0} | \mathbb{Q}_\phi^{x_0}) < \infty$  under the assumption that  $e(\phi) < \infty$ . As this implies  $\mathbb{P}^{x_0}$  is absolutely continuous with respect to  $\mathbb{Q}_\phi^{x_0}$ , the event  $Z_T = x_0$  holds  $\mathbb{Q}_\phi^{x_0}$ -almost surely as it is the case under  $\mathbb{P}^{x_0}$ .  $\square$

*Proof of Proposition 2.* By expanding the square in (12), we can decompose the Kullback–Leibler divergence as

$$\text{KL}(\mathbb{P}^{x_0} | \mathbb{Q}_\phi^{x_0}) = C_1 + C_2 - C_3, \quad (13)$$

where

$$\begin{aligned} C_1 &= \frac{1}{2} \int_0^T \|s(t, x_t)\|_{\Sigma(t, x_t)}^2 p(t, x_t | 0, x_0) dx_t dt, \\ C_2 &= \frac{1}{2} \sum_{m=1}^M \int_{t_{m-1}}^{t_m} \int_{\mathbb{R}^d} \|s_\phi(t, x_t)\|_{\Sigma(t, x_t)}^2 p(t, x_t | 0, x_0) dx_t dt, \\ C_3 &= \sum_{m=1}^M \int_{t_{m-1}}^{t_m} \int_{\mathbb{R}^d} \langle s_\phi(t, x_t), s(t, x_t) \rangle_{\Sigma(t, x_t)} p(t, x_t | 0, x_0) dx_t dt. \end{aligned} \quad (14)$$

We examine the term  $C_3$  that depends on the unknown score function  $s(t, x_t)$ . Firstly, we can write

$$C_3 = \sum_{m=1}^M \int_{t_{m-1}}^{t_m} \int_{\mathbb{R}^d} \langle s_\phi(t, x_t), \nabla p(t, x_t | 0, x_0) \rangle_{\Sigma(t, x_t)} dx_t dt.$$

By differentiating the Chapman–Kolmogorov equation with respect to the variable  $x_t$

$$\begin{aligned}\nabla p(t, x_t \mid 0, x_0) &= \nabla \int_{\mathbb{R}^d} p(t, x_t \mid t_{m-1}, x_{t_{m-1}}) p(t_{m-1}, x_{t_{m-1}} \mid 0, x_0) dx_{t_{m-1}} \\ &= \int_{\mathbb{R}^d} \nabla \log p(t, x_t \mid t_{m-1}, x_{t_{m-1}}) p(t, x_t \mid t_{m-1}, x_{t_{m-1}}) p(t_{m-1}, x_{t_{m-1}} \mid 0, x_0) dx_{t_{m-1}},\end{aligned}$$

we obtain

$$C_3 = \sum_{m=1}^M \int_{t_{m-1}}^{t_m} E^{x_0} \left\{ \left\langle s_\phi(t, X_t), \nabla \log p(t, X_t \mid t_{m-1}, X_{t_{m-1}}) \right\rangle_{\Sigma(t, X_t)} \right\} dt. \quad (15)$$

By expanding the square in (8) and using (14), (15), and

$$C_4 = \frac{1}{2} \sum_{m=1}^M \int_{t_{m-1}}^{t_m} E^{x_0} \left\{ \|g(t_{m-1}, X_{t_{m-1}}, t, X_t)\|_{\Sigma(t, X_t)}^2 \right\} dt,$$

we have

$$L(\phi) = C_2 - C_3 + C_4.$$

The claim follows by noting the decomposition in (13) and taking  $C = C_1 - C_4$ .  $\square$

## B Learning Doob’s $h$ -transform

Suppose we have found a minimizer  $\hat{\phi} \in \arg \min_{\phi \in \Phi} L(\phi)$  satisfying  $e(\hat{\phi}) < \infty$  and denote the corresponding score approximation as  $\hat{s}(t, x_t) = s_{\hat{\phi}}(t, x_t)$  and drift function as  $\hat{b}(t, z_t) = b_{\hat{\phi}}(t, z_t)$ . Consider a time-reversed bridge process  $\hat{Z} = (\hat{Z}_t)_{t \in [0, T]}$  satisfying

$$d\hat{Z}_t = \hat{b}(t, \hat{Z}_t) dt + \sigma(T - t, \hat{Z}_t) dB_t, \quad \hat{Z}_0 = x_T, \quad (16)$$

which should be seen as an approximation of (4). Let  $\hat{q}(t, z_t \mid s, z_s)$  denote its transition density for any  $0 \leq s < t \leq T$ ,  $\hat{\mathbb{Q}}^{x_0, x_T}$  be the induced path measure, and  $\hat{E}^{x_0, x_T}$  to denote expectation with respect to  $\hat{\mathbb{Q}}^{x_0, x_T}$ . Note that  $\hat{p}^*(t, x_t) = \hat{q}(T - t, x_t \mid 0, x_T)$  is an approximation of the marginal density  $p^*(t, x_t)$  in (5) for each  $t \in (0, T)$ .

Our discussion in (10) prompts having the time-reversal of (16) as an approximation of the Doob’s  $h$ -transform process  $X^*$  in (2). The bridge process  $\hat{X} = (\hat{X}_t)_{t \in [0, T]} = (\hat{Z}_{T-t})_{t \in [0, T]}$  satisfies

$$d\hat{X}_t = \hat{f}(t, \hat{X}_t) dt + \sigma(t, \hat{X}_t) dW_t, \quad \hat{X}_0 = x_0,$$

with drift function  $\hat{f}(t, x_t) = -\hat{b}(T - t, x_t) + \Sigma(t, x_t) \hat{s}^*(t, x_t) + \nabla \cdot \Sigma(t, x_t)$  which is to be seen as an approximation of  $f^*(t, x_t)$ . We can approximate the score  $\hat{s}^*(t, x_t) = \nabla \log \hat{p}^*(t, x_t)$  of the marginal density  $\hat{p}^*(t, x_t)$  and hence the time-reversal of (16) using the methodology described in Section 2.2. The following summarizes the key elements involved.

Consider a path measure  $\hat{\mathbb{Q}}_\phi^{x_0, x_T}$  that is induced by the bridge process  $\hat{X} = (\hat{X}_t)_{t \in [0, T]}$  satisfying

$$d\hat{X}_t = \hat{f}_\phi(t, \hat{X}_t)dt + \sigma(t, \hat{X}_t)dW_t, \quad \hat{X}_0 = x_0, \quad (17)$$

with drift function  $\hat{f}_\phi(t, x_t) = -\hat{b}(T - t, x_t) + \Sigma(t, x_t)\hat{s}_\phi^*(t, x_t) + \nabla \cdot \Sigma(t, x_t)$ , where  $\hat{s}_\phi^* : [0, T] \times \mathbb{R}^d \rightarrow \mathbb{R}^d$  denotes a function approximation of the score  $\hat{s}^*(t, x_t)$  with parameters  $\phi \in \Phi$  to be optimized. We now measure the score approximation error as

$$\hat{e}(\phi) = \hat{E}^{x_0, x_T} \left\{ \int_0^T \left\| \hat{s}_\phi^*(t, \hat{X}_t) - \hat{s}^*(t, \hat{X}_t) \right\|_{\Sigma(t, \hat{X}_t)}^2 dt \right\}.$$

**Proposition 3.** *Assuming  $\hat{e}(\phi) < \infty$ , we have  $\text{KL}(\hat{\mathbb{Q}}_\phi^{x_0, x_T} | \hat{\mathbb{Q}}_\phi^{x_0, x_T}) = \hat{e}(\phi)/2$  and  $\hat{X}_T = x_T$  holds  $\hat{\mathbb{Q}}_\phi^{x_0, x_T}$ -almost surely.*

**Proposition 4.** *For any partition  $(t_m)_{m=0}^M$  of the interval  $[0, T]$ , we have  $\text{KL}(\hat{\mathbb{Q}}_\phi^{x_0, x_T} | \hat{\mathbb{Q}}_\phi^{x_0, x_T}) = \hat{L}(\phi) + \hat{C}$  if  $\hat{e}(\phi) < \infty$ , where  $\hat{C}$  is a constant independent of  $\phi \in \Phi$ , the loss function is defined as*

$$\hat{L}(\phi) = \frac{1}{2} \sum_{m=1}^M \int_{t_{m-1}}^{t_m} \hat{E}^{x_0, x_T} \left\{ \left\| \hat{s}_\phi^*(T - t, \hat{Z}_t) - \hat{g}(t_{m-1}, \hat{Z}_{t_{m-1}}, t, \hat{Z}_t) \right\|_{\Sigma(t, \hat{Z}_t)}^2 \right\} dt, \quad (18)$$

and  $\hat{g}(s, z_s, t, z_t) = \nabla \log \hat{q}(t, z_t | s, z_s)$  for  $0 \leq s < t \leq T$  and  $z_s, z_t \in \mathbb{R}^d$ .

The proof of these results is similar to Appendix A and is thus omitted. As before, this allows us to circumvent intractability in the Kullback–Leibler divergence  $\text{KL}(\hat{\mathbb{Q}}_\phi^{x_0, x_T} | \hat{\mathbb{Q}}_\phi^{x_0, x_T})$  by minimizing the loss function  $\hat{L}(\phi)$ . In the ideal case of  $\hat{s}_\phi^*(t, x_t) = \hat{s}^*(t, x_t)$   $\hat{\mathbb{Q}}_\phi^{x_0, x_T}$ -almost surely, the minimal loss of  $\hat{L}(\phi) = -\hat{C}$  is also unknown in practice, and  $\hat{\mathbb{Q}}_\phi^{x_0, x_T}$  recovers the law of the diffusion bridge process  $X^*$  only if the initial score approximation error satisfies  $e(\hat{\phi}) = 0$ .

Given a minimizer  $\phi^\circ \in \arg \min_{\phi \in \Phi} \hat{L}(\phi)$  and the corresponding score approximation  $s^\circ(t, x_t) = \hat{s}_{\phi^\circ}^*(t, x_t)$ , by rewriting the drift  $f^\circ(t, x_t) = \hat{f}_{\phi^\circ}(t, x_t)$  as

$$f^\circ(t, x_t) = f(t, x_t) + \Sigma(t, x_t)\{s^\circ(t, x_t) - \hat{s}(t, x_t)\}$$

and comparing it with (10), we see that the last two terms on the right provide an approximation of the term  $\Sigma(t, x_t)\nabla \log h(t, x_t)$  in Doob’s  $h$ -transform.

## C Numerical implementation

In this section, we detail various numerical considerations to implement our proposed methodology. For simplicity, we employ the Euler–Maruyama scheme (Kloeden and Platen, 1992, p. 340) on a uniform discretization of the interval  $[0, T]$ , denoted by  $0 = t_0 < t_1 < \dots < t_M = T$ , with stepsize  $\delta t = T/M$  for  $M > 1$ . Non-uniform discretizations involve only minor modifications; some higher-order schemes could also be considered. In the following, we denote a multivariate normal distribution with mean vector  $\mu \in \mathbb{R}^d$  and covariance matrix  $\Sigma \in \mathbb{R}^{d \times d}$  as  $\mathcal{N}(\mu, \Sigma)$ , and its density as  $x \mapsto \mathcal{N}(x; \mu, \Sigma)$ . We write the zero vector as  $0_d \in \mathbb{R}^d$  and the identity matrix as  $I_d \in \mathbb{R}^{d \times d}$ .

The time-discretization of the stochastic differential equation defining  $X$  satisfies the following recursion

$$X_{t_m} = X_{t_{m-1}} + \delta t f(t_{m-1}, X_{t_{m-1}}) + \sigma(t_{m-1}, X_{t_{m-1}})(W_{t_m} - W_{t_{m-1}}), \quad X_0 = x_0, \quad (19)$$

for  $m \in \{1, \dots, M\}$ , with independent Brownian increments  $W_{t_m} - W_{t_{m-1}} \sim \mathcal{N}(0_d, \delta t I_d)$ . Equation (19) induces a normal approximation of the transition density  $p(t_m, x_{t_m} \mid t_{m-1}, x_{t_{m-1}})$  of the form

$$p_M(t_m, x_{t_m} \mid t_{m-1}, x_{t_{m-1}}) = \mathcal{N}\{x_{t_m}; x_{t_{m-1}} + \delta t f(t_{m-1}, x_{t_{m-1}}), \delta t \Sigma(t_{m-1}, x_{t_{m-1}})\}.$$

By replacing the score of  $p(t_m, x_{t_m} \mid t_{m-1}, x_{t_{m-1}})$  with that of  $p_M(t_m, x_{t_m} \mid t_{m-1}, x_{t_{m-1}})$ , the gradient  $g(t_{m-1}, x_{t_{m-1}}, t_m, x_{t_m})$  in Proposition 2 can be approximated by

$$g_M(t_{m-1}, x_{t_{m-1}}, t_m, x_{t_m}) = -(\delta t)^{-1} \Sigma^{-1}(t_{m-1}, x_{t_{m-1}}) \{x_{t_m} - x_{t_{m-1}} - \delta t f(t_{m-1}, x_{t_{m-1}})\}.$$

We then define the following approximation of the loss function  $L(\phi)$  in (8)

$$L_M(\phi) = \frac{1}{2} \delta t \sum_{m=1}^M E_M^{x_0} \left\{ \left\| s_\phi(t_m, X_{t_m}) - g_M(t_{m-1}, X_{t_{m-1}}, t_m, X_{t_m}) \right\|_{\Sigma(t_m, X_{t_m})}^2 \right\},$$

where  $E_M^{x_0}$  denotes expectation with respect to the law of the time-discretized process under (19). To obtain a minimizer  $\hat{\phi} \in \arg \min_{\phi \in \Phi} L_M(\phi)$  using stochastic gradient algorithms, the gradient with respect to parameters  $\phi \in \Phi$

$$\nabla_\phi L_M(\phi) = \delta t \sum_{m=1}^M E_M^{x_0} \left[ (\nabla_\phi s_\phi^\top \Sigma)(t_m, X_{t_m}) \{s_\phi(t_m, X_{t_m}) - g_M(t_{m-1}, X_{t_{m-1}}, t_m, X_{t_m})\} \right] \quad (20)$$

can be unbiasedly estimated using independent sample paths from (19). The above notation  $\nabla_\phi s_\phi$  refers to the Jacobian of  $s_\phi$ . Equation (20) can be seen as an approximation of the gradient  $\nabla_\phi L(\phi)$ .

After obtaining  $\hat{\phi}$  with optimization, we can simulate a proposal bridge  $\hat{Z} = (\hat{Z}_t)_{t \in [0, T]}$  satisfying (16) with drift function  $\hat{b}(t, z_t) = b_{\hat{\phi}}(t, z_t)$ . We employ the following modified Euler–Maruyama scheme

$$\hat{Z}_{t_m} = \hat{Z}_{t_{m-1}} + \delta t \hat{b}(t_{m-1}, \hat{Z}_{t_{m-1}}) + \left( \frac{T - t_m}{T - t_{m-1}} \right)^{1/2} \sigma(T - t_{m-1}, \hat{Z}_{t_{m-1}}) (B_{t_m} - B_{t_{m-1}}), \quad (21)$$

for  $m \in \{1, \dots, M-1\}$ , with independent Brownian increments  $B_{t_m} - B_{t_{m-1}} \sim \mathcal{N}(0_d, \delta t I_d)$ , initial condition  $\hat{Z}_0 = x_T$ , and terminal constraint  $\hat{Z}_T = x_0$ . This changes the variance of the usual Euler–Maruyama transitions with a multiplier of  $(T - t_m)/(T - t_{m-1})$  at time step  $m$ . We found that this modification can improve practical performance for times near the endpoint by lowering the transition variances. Such behaviour is consistent with findings in earlier works by [Durham and Gallant \(2002\)](#) and [Papaspiliopoulos et al. \(2013\)](#) when constructing proposal bridge processes with the drift of a Brownian bridge. This gives a normal approximation of the transition density  $\hat{q}(t_m, z_{t_m} \mid t_{m-1}, z_{t_{m-1}})$

$$\begin{aligned} & \hat{q}_M(t_m, z_{t_m} \mid t_{m-1}, z_{t_{m-1}}) \\ &= \mathcal{N} \left\{ z_{t_m}; z_{t_{m-1}} + \delta t \hat{b}(t_{m-1}, z_{t_{m-1}}), \delta t \left( \frac{T - t_m}{T - t_{m-1}} \right) \Sigma(T - t_{m-1}, z_{t_{m-1}}) \right\}. \end{aligned} \quad (22)$$

We can perform importance sampling on  $\mathbb{E}_M = (\mathbb{R}^d)^{M-1}$  to correct for the discrepancy between the law of our proposal bridge process

$$\hat{Q}_M^{x_0, x_T}(z_{t_1:t_{M-1}}) = \prod_{m=1}^{M-1} \hat{q}_M(t_m, z_{t_m} \mid t_{m-1}, z_{t_{m-1}}), \quad z_{t_1:t_{M-1}} = (z_{t_m})_{m=1}^{M-1} \in \mathbb{E}_M, \quad (23)$$

and the law of the time-discretized diffusion bridge process

$$P_M^{x_0, x_T}(x_{t_1:t_{M-1}}) = \frac{\gamma_M^{x_0, x_T}(x_{t_1:t_{M-1}})}{p_M(T, x_T \mid 0, x_0)}, \quad x_{t_1:t_{M-1}} = (x_{t_m})_{m=1}^{M-1} \in \mathbb{E}_M, \quad (24)$$

with  $\gamma_M^{x_0, x_T}(x_{t_1:t_{M-1}}) = \prod_{m=1}^M p_M(t_m, x_{t_m} \mid t_{m-1}, x_{t_{m-1}})$ , and also estimate

$$p_M(T, x_T \mid 0, x_0) = \int_{\mathbb{E}_M} \gamma_M^{x_0, x_T}(x_{t_1:t_{M-1}}) dx_{t_1:t_{M-1}}, \quad (25)$$

which is an approximation of the transition density  $p(T, x_T \mid 0, x_0)$  under the Euler–Maruyama scheme. The corresponding unnormalized importance weight is

$$\omega(z_{t_1:t_{M-1}}) = \frac{\gamma_M^{x_0, x_T}(x_{t_1:t_{M-1}})}{\hat{Q}_M^{x_0, x_T}(z_{t_1:t_{M-1}})}$$

with  $x_{t_1:t_{M-1}} = (z_{T-t_m})_{m=1}^{M-1}$ , and an unbiased importance sampling estimator of the transition density  $p_M(T, x_T \mid 0, x_0)$  is  $N^{-1} \sum_{n=1}^N \omega(z_{t_1:t_{M-1}}^n)$  where  $(z_{t_1:t_{M-1}}^n)_{n=1}^N$  denote  $N \in \mathbb{N}$  independent sample paths from  $\hat{Q}_M^{x_0, x_T}$ . As noted by [Lin et al. \(2010\)](#), the root mean squared error of this transition density estimator is approximately equals to the  $\chi^2$ -divergence of  $\hat{Q}_M^{x_0, x_T}$  from  $P_M^{x_0, x_T}$  divided by the sample size  $N$ . One can also employ proposals from (23) within an independent Metropolis–Hastings algorithm that has (24) as its invariant law ([Elerian et al., 2001](#)). At each iteration of the algorithm, a sample path  $z_{t_1:t_{M-1}}^\circ \sim \hat{Q}_M^{x_0, x_T}$  is accepted with probability  $\min\{1, \omega(z_{t_1:t_{M-1}}^\circ)/\omega(z_{t_1:t_{M-1}})\}$ , where  $z_{t_1:t_{M-1}}$  denotes the current state of the Markov chain. The efficiency of this Markov chain Monte Carlo algorithm can be assessed by monitoring its acceptance probability. To improve the acceptance probability, we can also combine independent Metropolis–Hastings with importance sampling within a particle independent Metropolis–Hastings algorithm ([Andrieu et al., 2010](#)) that has invariant law (24). Each iteration of this algorithm involves selecting a proposed sample path  $z_{t_1:t_{M-1}}^\circ$  among  $N$  candidates  $(z_{t_1:t_{M-1}}^n)_{n=1}^N \sim \hat{Q}_M^{x_0, x_T}$  according to probabilities proportional to their weights  $(\omega(z_{t_1:t_{M-1}}^n))_{n=1}^N$ , and accepting it with probability  $\min\{1, \hat{p}_M^\circ(T, x_T \mid 0, x_0)/\hat{p}_M(T, x_T \mid 0, x_0)\}$  that depends on the ratio of the new and current transition density estimators  $\hat{p}_M^\circ(T, x_T \mid 0, x_0) = N^{-1} \sum_{n=1}^N \omega(z_{t_1:t_{M-1}}^n)$  and  $\hat{p}_M(T, x_T \mid 0, x_0)$ , respectively. Under mild assumptions, consistency of importance sampling estimators as  $N \rightarrow \infty$  implies that the acceptance probability of particle independent Metropolis–Hastings algorithm converges to one. This algorithm can also be combined with unbiased Markov chain Monte Carlo methods to provide unbiased estimates of expectations with respect to the law of the time-discretized diffusion bridge ([Middleton et al., 2019](#)).

Lastly, we sketch the key steps to learn the Doob’s  $h$ -transform process for the sake of brevity. Using the score of the normal transition density in (22), we may approximate  $\hat{g}(t_{m-1}, z_{t_{m-1}}, t_m, z_{t_m})$

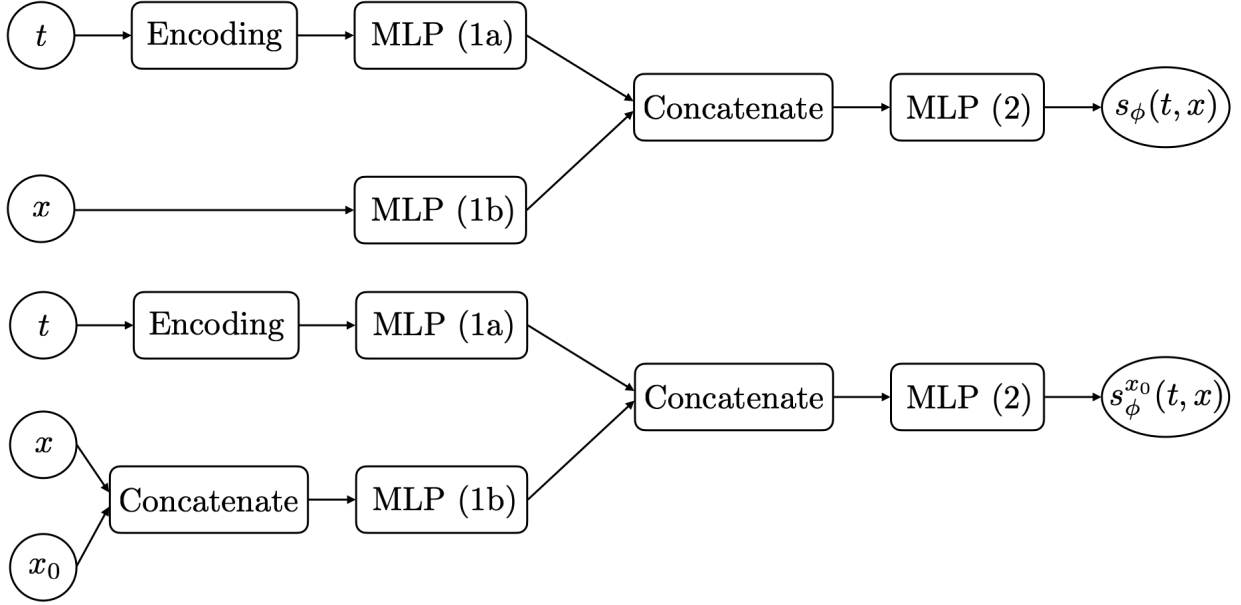


Figure 5: Neural network architectures involve multi-layer perceptron (MLP) blocks and an “Encoding” block which applies the sine transform described in Vaswani et al. (2017). MLP (1a) and (1b) have one hidden layer and MLP (2) has two hidden layers. All neurons use the Leaky ReLU activation function.

and hence the loss function  $\hat{L}(\phi)$  in (18). The approximate loss can be minimized using stochastic gradient algorithms and sample paths from (21). By time-discretizing the resulting proposal bridge process in (17), we may then employ it as an importance proposal to approximate the law in (24) and the transition density in (25), or to generate proposal distributions within independent Metropolis–Hastings algorithms.

## D Implementation details

### D.1 Neural network and stochastic optimization

The architecture of the neural networks we employed is illustrated in Fig. 5. For all numerical experiments, optimization was performed using the stochastic gradient algorithm of Kingma and Ba (2014) with a momentum of 0.99 and learning rate of 0.01.

### D.2 Ornstein–Uhlenbeck process

Let  $X$  be an Ornstein–Uhlenbeck process, defined by (1) with linear drift function  $f(t, x_t) = \alpha - \beta x_t$  and identity diffusion coefficient  $\sigma(t, x_t) = I_d$ . In this analytically tractable example, for any  $0 \leq s < t \leq T$ , the transition density of  $X$  is a normal density  $p(t, x_t \mid s, x_s) =$

$\mathcal{N}\{x_t; m(t-s, x_s), v(t-s)I_d\}$ , with the following mean and variance

$$m(t-s, x_s) = \frac{\alpha}{\beta} + \left(x_s - \frac{\alpha}{\beta}\right) \exp\{-\beta(t-s)\}, \quad v(t-s) = \frac{1 - \exp\{-2\beta(t-s)\}}{2\beta}.$$

Hence the logarithmic gradient term in the Doob's  $h$ -transform of (2) is

$$\nabla \log h(t, x_t) = \frac{\exp\{-\beta(T-t)\}}{v(T-t)} \{x_T - m(T-t, x_t)\},$$

and the score of the transition density in (4) is

$$s(t, x_t) = v(t)^{-1} \{m(t, x_0) - x_t\}.$$

For dimension  $d = 1$  and varying time horizon  $T \in \{1, 2, 4, 8\}$ , we employed a time-discretization stepsize of  $\delta t = 0.02$ , 500 optimization iterations, and 100 sample paths per iteration. For the case of  $T = 1$  and varying  $d \in \{1, 2, 4, 8\}$ , we decreased the stepsize and increased the number of optimization iterations and the capacity of the neural network with dimension.

### D.3 Interest rates model

We consider a special case of an interest rates model in [Ait-Sahalia and Lo \(1998\)](#), defined by (1) with drift function  $f(t, x_t) = \theta/x_t - x_t$  and diffusion coefficient  $\sigma(t, x_t) = 1$ . The transition density of this diffusion is known and given by

$$\begin{aligned} \log p(t, x_t | s, x_s) &= \theta \log(x_t/x_s) + \frac{1}{2} \log(x_t x_s) - x_t^2 + \left(\theta + \frac{1}{2}\right) (t-s) \\ &\quad - \log \sinh(t-s) - \frac{x_t^2 + x_s^2}{\exp\{2(t-s)\} - 1} + \log I_{\theta-1/2} \left\{ \frac{x_t x_s}{\sinh(t-s)} \right\}, \end{aligned}$$

for  $0 \leq s < t \leq T$ , where  $I_\nu$  denotes the modified Bessel function of order  $\nu$ . The logarithmic gradient term in the Doob's  $h$ -transform of (2) is

$$\begin{aligned} \nabla \log h(t, x_t) &= -\frac{\theta}{x_t} + \frac{1}{2x_t} - \frac{2x_t}{\exp\{2(T-t)\} - 1} \\ &\quad + I_{\theta-1/2} \left\{ \frac{x_T x_t}{\sinh(T-t)} \right\}^{-1} J_{\theta-1/2} \left\{ \frac{x_T x_t}{\sinh(T-t)} \right\} \frac{x_T}{\sinh(T-t)}, \end{aligned}$$

and the score of the transition density in (4) is

$$s(t, x_t) = \frac{\theta}{x_t} + \frac{1}{2x_t} - 2x_t - \frac{2x_t}{\exp(2t) - 1} + I_{\theta-1/2} \left\{ \frac{x_t x_0}{\sinh(t)} \right\}^{-1} J_{\theta-1/2} \left\{ \frac{x_t x_0}{\sinh(t)} \right\} \frac{x_0}{\sinh(t)},$$

where  $J_\nu$  denotes the derivative of  $I_\nu$ .

Numerical experiments for all  $T \in \{1, 2, 4, 8\}$  employed a time-discretization stepsize of  $\delta t = 0.02$ , 1000 optimization iterations, 1000 sample paths per iteration with 10 unique initial conditions  $X_0 = x_0$  sampled from the gamma distribution with shape 5 and rate 2.

### D.4 Cell model

Our numerical experiments for all  $T \in \{2, 4, 8, 16\}$  and  $\sigma_X^2 \in \{0.1, 1\}$  employed a time-discretization stepsize of  $\delta t = 0.02$ , 2000 optimization iterations, and 100 sample paths per iteration.